



A Novel Redundant Continuum Manipulator with Variable Geometry Trusses

Wenxiang Zhao and Wenzeng Zhang^(✉)

Department of Mechanical Engineering, Tsinghua University, Beijing 100084, China
wenzeng@tsinghua.edu.cn

Abstract. This paper proposed a kind of variable geometry trussed (VGT) redundant continuum manipulators, which are a type of super-redundant robot. Compared to traditional robots, this robot has many advantages such as high rigidity, modularity, and flexibility. Due to these advantages, the VGT redundant continuum manipulators can be applied in remote control of space, underwater detection, and an industrial environment with obstacles. Besides, due to its deformable characteristics, it can also be used as a logging tractor to adaptively move in unstructured pipeline installations. This paper introduces a modular concept and considers the symmetry of the single-module robot during the construction process, which simplifies the kinematics calculation of a complex robot into a kinematics calculation of a single module, and makes this robot's kinematics' solutions be derived from the geometric relationships of the model explicitly. At the same time, due to the modular design, the robotic arm has a wide range of applications in the future.

Keywords: Manipulator · Ultra-redundant · Variable Geometry Truss Modular

1 Introduction

Since the first industrial robot was built in the United States in 1952 [1], the robot has developed very rapidly and has been widely used in many fields such as the automobile, the electronics, the nuclear and the service industry. Nowadays the robot configuration can generally be divided into series configurations and parallel configurations, and both of them have advantages and disadvantages.

The first to use in industrial production was a serial robot. In 1958 [2], Joseph F. Engel Berger, known as the “father of industrial robots,” created the world's first robot company, Unimentation (Universal Automation), and participated in the design of the first Unimate robot. This is a 5-axis hydraulically driven robot for die casting and the control system is operated by just one computer [3]. It is mainly used for material transport between machines, which can rotate around the base and move up and down in the vertical direction. The Unimate robots are generally

considered to be the earliest industrial robots in the world. And now the series robots are also on the basis of these two robots on evolved.

In 1978, Hunt, a renowned institutional professor from Australia, proposed the Stewart platform mechanism which has six-degrees of freedom as a robotic mechanism, which is the origin of the concept of parallel robots [4]. A typical Stewart parallel mechanism consists of six independent and freely retractable struts, which are connected by a ball joint and a Hooke hinge. In this way, the upper platform and the lower platform have 6 independent motions and 6 degrees of freedom, which makes it can be moved in any direction and rotated about any axis in any direction or position.

With the development of science and technology, both of the two structures have been widely used. However, both configurations have their inevitable drawbacks.

For example, the axes of the series robots need to be controlled independently with corresponding encoders and sensors, which makes their control is difficult, and they are prone to have dynamic errors and cumulative errors [5]. In addition, the large working space would cause a large inertia. Although the parallel robot does not have the above problems, its motion analysis is complicated and there is a coupling effect between the drive axes. The most serious problem is that the working space of parallel robots is relatively small which makes them mostly used for a small working table and cannot handle large-sized parts [6].

At the end of the 1990s, the research of the hybrid mechanism gradually attracted people's attention. The hybrid mechanism is expected to integrate the advantages of parallel robots and series robots, which is a new development direction of robot. In 1994, Husain conducted a research on the positional dynamics of a three-branch hybrid platform mechanism. In 1999, the Shenyang Institute of Automation also successfully developed a five-axis machine tool (four-axis parallel, one-axis series). Research on hybrid machine has become a hot topic [7].

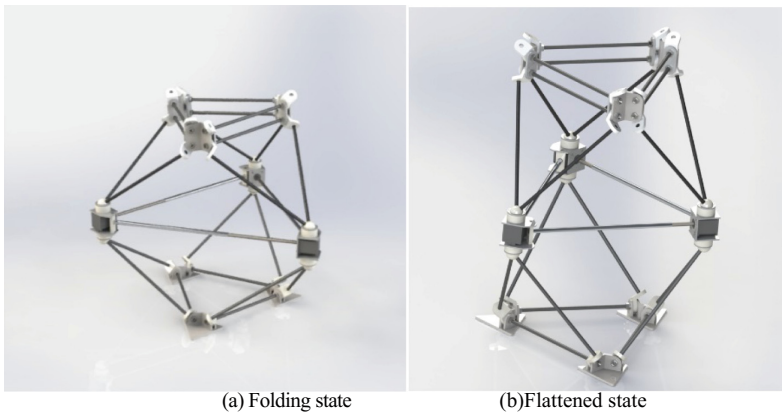


Fig. 1. The different forms of VGT manipulators unit modular

Based on this background, this paper hopes to overcome the above-mentioned problems through the modular design based on the two structures. Utilizing the advantages

of the truss mechanism and the axial force characteristics and the high stiffness to mass ratio, the robot can significantly increase the load capacity and positioning accuracy. VGT continuum manipulator came into being (Fig. 1).

2 The Principle of Design and Motion

2.1 The Principle of Design

The overall structure is similar to that of the Stewart platform, but the driving is to change the position and direction of the target plane by changing the side length of the triangle of the active layer to drive the movement of the mechanism. In contrast, the traditional Stewart platform does not have an efficient inverse motion solution currently. However, this design can use the length of each side of the active layer to accurately solve the position and direction of the work plane, so as to achieve accurate motion control [10].

The active layer changes the length of each side and drives the linkage movement. The passive layer realizes the series connection of each unit body, and the active layer and the passive layer are arranged alternately. When one actuator of the active layer is extended, the two triangles connected to it are changed to an obtuse triangle, and the height of the base is reduced, so that the unit body is bent toward the actuator, and the two passive planes are opposite to each other as shown in Fig. 2.

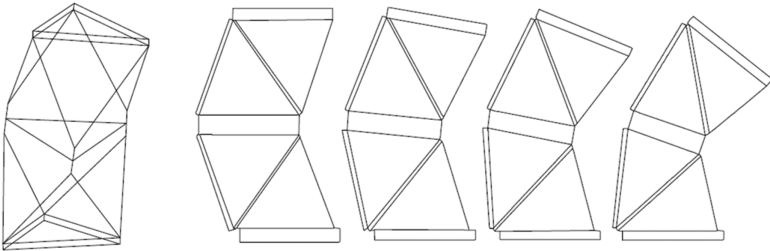


Fig. 2. The formation of a modular and .manipulators

The adjustment range of a unit body is relatively limited, but in the case of multiple unit bodies connected in series, not only has a large movement reachable space, but also can achieve a variety of functions such as motion path planning, as shown in Fig. 3.

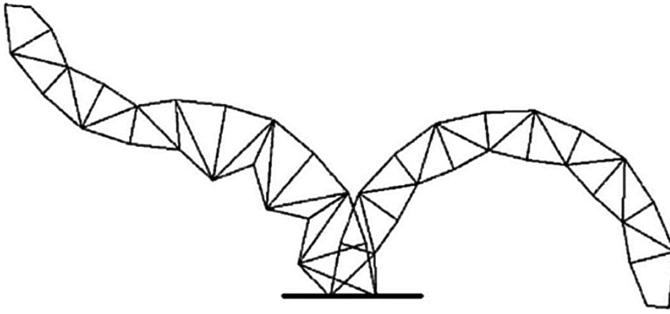


Fig. 3. The formation of the series manipulators

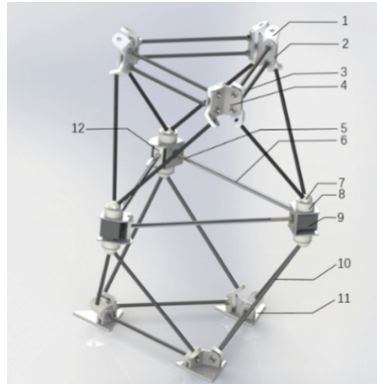
2.2 The Principle of Motion

Based on the above motion analysis, the original multi-degree-of-freedom spherical hinge can be simplified accordingly, taking into account that the scope of the sphere hinge is mechanically smaller as well as a certain gap, so that in the actual design, we dismantled the ball joint into a rotating hinge and a universal joint to achieve three rotational degrees of freedom. The degree of freedom is calculated that $S = 3$ which is consistent with the original design goals using the GrUbler-Kutzbach formula, where component N is taken as 14, and each rod in the active layer can be split into two components. The number of motion pairs and the degree of freedom are calculated as shown in Table 1 below [8, 9].

Table 1. The calculation of degree-of-freedom

Kinetic pair	Number	Degrees of freedom
Revolute pair in passive layer	6	1
Sphere-trough pair in active layer	6	3
Linear pair in active layer	3	2
Revolute pair in active layer	3	1

Due to the high requirements for accuracy and light weight, we finally choose the driving pattern of the motor plus screw, which achieves the purpose of reducing the weight (Fig. 4).



1-revolute pair; 2-mounting plate; 3-mounting rod; 4-connecting plate; 5-screw; 6-active rod; 7, 8-spherical hinge; 9-stepper motor; 10-connecting rod; 11-base panel; 12-active layer revolute pair

Fig. 4. The main assembly of VGT manipulators

3 Architecture of the VGT Manipulators

3.1 Main Assembly

According to actual demand in applications, a complete VGT redundant continuum manipulators can be composed of a different number of unit modules, so this paper only analyze one unit module. A unit module is divided into two passive layers and one active layer. The active layer consists of three stepping motors connected to three leadscrew to form a triangle. Each stepper motor uses 12 V DC to work independently. The screw rotates the motor into a telescopic motion, causing the two triangles connected to it to change. The unit body bends while the two passive layers rotate relative to each other. The three motors are independent of each other, so that the two passive planes have three relative generalized degrees of freedom.

3.2 The Architecture of Active Layer

The active layer consists of three drive units that form a triangle. Each drive unit includes a stepper motor, a motor bracket, a screw, a sleeve, and two universal joints. The motor bracket is mainly used to fix the motor and connect the universal joint and the sleeve connector together. The stepper motor connects to the lead screw and provides torque to rotate the lead screw. One end of the sleeve connects to the motor bracket through a connector that can rotate relative to the bracket, and the other end sleeves on the screw. The two revolute pair on each universal joint provide two degrees of freedom. The universal joint connects to the passive layer by two linkages, so that the two linkages and the passive layer form an equilateral triangle with a fixed side length (Fig. 5).

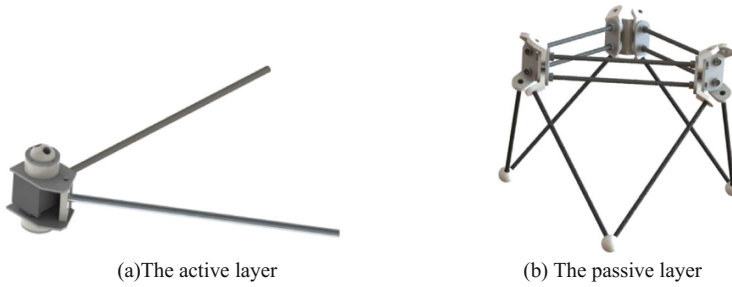


Fig. 5. The architecture of active layer and passive layer

3.3 The Architecture of Passive Layer

The passive layer includes three fixed-length passive layer linkages and three connectors. The two adjacent linkages and the passive layer linkages on the two connecting members form an equilateral triangle, which can rotate about the passive layer connecting members under the action of the rotating pair on the connectors.

3.4 Motion Control System

In terms of motion control, we make it through communication between *Arduino* and *Matlab*. By giving the length of three rods, we can achieve the positive kinematics control. And by giving the end of the three coordinate values, we can also achieve inverse kinematics control. In addition, it also achieve the round path, straight path, polygonal path and other functions of the end coordinates. After calculation, Matlab pass predetermined three lengths of information to the Arduino to control. On the one hand, reducing the Arduino's computational burden, on the other hand, it makes it possible to implement multiple motion modes of the module.

The prime mover is stepper motors whose step angle is 1.8° with 8 mm lead screw, which make the control precision to 0.04 mm, achieving the desired accuracy. At the same time, among the modules of multiple units, we select the motor with the larger torque in the bottom module, while the motor with the small torque but light is in the top module to achieve a balanced state.

The final unit structure can achieve various movements and accurately reach any position in space, which achieve the desired goal, shown as Fig. 6.

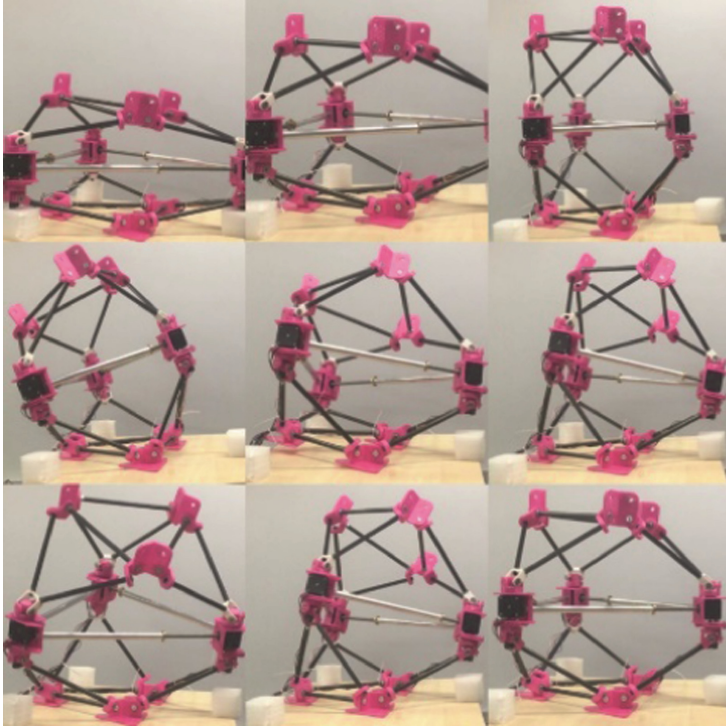


Fig. 6. The flexible deformation of a unit modular

4 Analysis of the VGT Manipulators

4.1 Kinematic Analysis

As shown in the Fig. 7 below, the module is regarded as a combination of two symmetrical octahedral truss structures [11]. The part in which the actuator directly control is a common symmetry plane M (active layer), including triangles G_1, G_2, G_3 composed of three length-adjustable sides l_{12}, l_{23}, l_{31} . The plane opposite to the plane M in each octahedral truss structure is defined as the bottom surface B and the top surface P (passive layer), and the centers of these two planar triangles are O and O_i respectively.

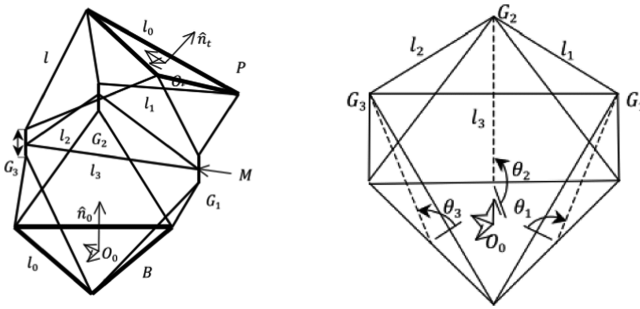


Fig. 7. The simplified octahedron model diagram

For the positive kinematics problem of the module unit, we need to calculate the coordinates of the center point O_i of the end plane through the length of the three active bars. That is, the input variables for positive kinematics are l_{12}, l_{23}, l_{31} , and the output variable is OO_i .

We introduce the plane angles $\theta_1, \theta_2, \theta_3$ of the three planes and the bottom plane as the intermediate variables that link the input variables with the output variables, as shown in the Fig. 7 above.

To simplify the expression, noting that $N = \sqrt{l_s^2 - l^2/4}$, then the coordinates of the bottom three sides can be expressed as

$$O_1 = \left[-\frac{l}{2\sqrt{3}}, 0, 0 \right] \tag{1}$$

$$O_2 = \left[\frac{l}{4\sqrt{3}}, -\frac{l}{4}, 0 \right] \tag{2}$$

$$O_3 = \left[\frac{l}{4\sqrt{3}}, \frac{l}{4}, 0 \right] \tag{3}$$

Then we can get the coordinates of the actuator plane's vertices G_1, G_2, G_3 :

$$G_1 = \left[-\frac{l}{2\sqrt{3}} + N\cos\theta_1, 0, N\sin\theta_1 \right] \tag{4}$$

$$G_2 = \left[\frac{l}{4\sqrt{3}} - \frac{N}{2}\cos\theta_2, -\frac{l}{4} + \frac{\sqrt{3}Nc_2}{2}, N\sin\theta_2 \right] \tag{5}$$

$$G_3 = \left[\frac{l}{4\sqrt{3}} - \frac{N}{2} \cos\theta_3, \frac{l}{4} - \frac{\sqrt{3}Nc_3}{2}, N\sin\theta_3 \right] \tag{6}$$

So that we can get the concrete expression

$$\begin{aligned} & \left(3k^2 + 2 - \left(\frac{l_{ij}}{N} \right)^2 \right) \sqrt{1 + \tan^2\theta_i} \sqrt{1 + \tan^2\theta_j} \\ & = \pm 3k \left(\sqrt{1 + \tan^2\theta_i} + \sqrt{1 + \tan^2\theta_j} \right) - 1 + 2\tan\theta_i \tan\theta_j, \\ & \quad i, j = 1, 2, 3 \dots i \neq j \end{aligned} \tag{7}$$

Among them

$$k = \frac{l}{2\sqrt{3}N}$$

According to the geometric relation of the following figure, under the condition of solving $\theta_1, \theta_2, \theta_3$, the coordinates of O_i can be expressed as (Fig. 8):

$$O_i = (2G_i \cdot \vec{n} + s) \vec{n} \tag{8}$$

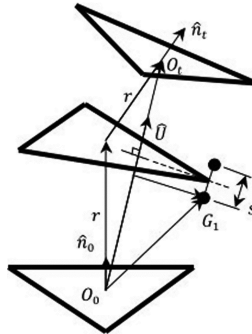


Fig. 8. The geometric relation of O_0 and O_i

4.2 Mechanical Analysis

After the design of the mechanism was completed, we used ANSYS to analyze the force under the action of its own weight and the load of 1 kg under the top. In order to simplify the model, we consider the nodes as rigid bodies and concentrate the mass of the rods on the nodes. The material settings correspond to the actual situation. According to the data, the bending strength and tensile strength of 3 K carbon fiber tubes are all 1500 MPa [12]. In order to check the carrying condition of the mechanism under the limit state,

suppose there is no suspension system now, only the base support. The model and calculation results are realized in the form of a histogram, as shown in the Fig. 9.

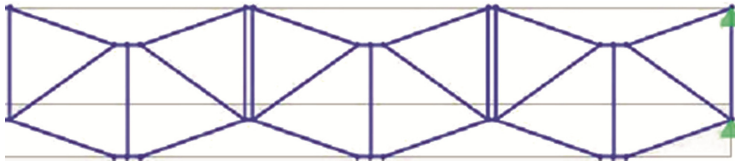


Fig. 9. The model of mechanical analysis.

We specify that in each small triangle, the left rod is the rod 1, the upper rod is the rod 2, and the lower rod is the rod 3. Due to the symmetrical structure, there are six different sets of members subjected to the force in the above figure. Now the six sets of members are subjected to the force in the form of a histogram as follows (Fig. 10):

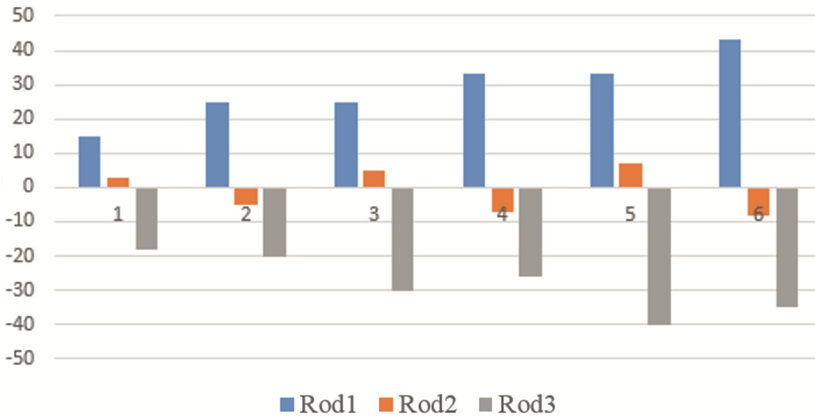


Fig. 10. Image of stress of each rod.

According to calculations, the force applied to the end member will not exceed 50 N. Since the diameter of the selected carbon fiber tube is 10 mm and the wall thickness is 1 mm, the maximum stress is calculated as

$$\delta = -\frac{M \times y}{I} = -\frac{F \times l \times \frac{d_1}{2}}{\frac{\pi(d_1^4 - d_2^4)}{64}} = 172 \text{ Mpa} \ll [\delta] = 1500 \text{ Mpa}$$

It can be seen that the strength of the structure meets the requirements at any time.

4.3 Experiments of Moduler Unit

In order to test the precision of the product when adjusting the position, we conducted a preliminary test on the manipulator. The test process are the following, a space rectangular coordinate system is established with the center of the ground triangle as the origin, and the coordinates of the center point of the top triangle are used as the measurement elements. We randomly select 9 sets of coordinates, and through theoretical calculations, we obtain the length of each side of the active layer needed to position the center point of the top triangle at this target. Using this calculation result as a parameter, combined with the plumb line and other tools to measure, get the actual coordinates of the center point, compared with the theoretical coordinates selected in advance, and analyze the error. Repeat 9 sets of experiments to get theoretical coordinates and actual coordinates and their errors are as Table 2.

Table 2. The comparison of expected and actual coordinates

Target coordinates/mm			Actual coordinates/mm			Relative error/%
X	Y	Z	X	Y	Z	
0	0	253	0	0	250	1.186
0	0	340	0	3	334	1.973
0	0	400	0	6	394	2.121
30	0	330	26	4	319	3.733
0	60	350	3	55	342	2.788
20	60	350	16	52	344	3.028
100	0	300	89	-6	289	5.273
0	120	290	-6	110	278	5.332
100	100	300	92	108	292	4.178

The test results show that the relative error between the actual coordinates and the theoretical coordinates is within 6%, which is in an acceptable range.

The main causes of the error are:

- (a) The accuracy of the connector obtained by 3D printing is low, and there is a certain error in the assembly process;
- (b) The stiffness of the connector by 3D printing is small, and when the force is applied, a certain deformation and bending would occur;
- (c) Some measurement errors occurs;
- (d) Stepper motors have lost motion during operation.

5 The Application of VGT Manipulators

The structure maintains an indeterminate structure at any location, with high stiffness and light weight. After measurement, the total weight of one module is only 1.8 kg, the weight of two modules will not exceed 5 kg, and the movement range of the two modules also reaches 0.6 m. Compared with traditional series robots, the manipulator can achieve

a greater range of motion [13]. From the above-mentioned mechanical analysis, it can be seen that in all motion ranges, a certain degree of strength can be ensured, which has a wide range of application values.

- (1) The manipulators can be used as a support for a solar-powered windsurfing space deployment mechanism, which can be folded and saved space before it occurs. In space, fine-tuning the motor parameters can make the solar-powered windsurfing always stay at the best position.
- (2) The manipulator can be developed as a pipeline robot [14]. The pipeline robot is composed of multiple modules. Rollers are added to the nodes of several active layers and the length of each side of the active layer can be freely adjusted within a certain range to ensure that the rollers are in close proximity to the pipe wall. Because the adjustment of the length of the active layer is relatively simple, this product can be automatically adapted to pipes of different diameters after modification. Refitted pipe robots can be used in pipeline inspection and maintenance operations. Traditional pipeline robots are difficult to adapt to complex pipelines with large changes in pipe diameter, but pipeline robots made with VGT structures can better adapt to complex pipelines.
- (3) The manipulator has a strong scalability and large potential in development. The unit modules can not only design as octahedron VGTs, but also can be extended to decahedrons, dodecahedrons, etc. When the number of facets of the unit modules is larger, the movement that the manipulator can achieve becomes more complicated.

6 Conclusions

This paper proposed a variable geometry trussed redundant continuum manipulator with the advantages of serial robots and parallel robots, which effectively solved the inherent defects of various types of robots in modern industrial production. Using a modular parallel mechanism and connecting multiple modules in series, achieves complex space motion while ensuring high accuracy [15].

As mentioned by related scholars above, the possibility of ultra-redundant robots can only be limited by imagination.

Acknowledgement. This Research was supported by National Natural Science Foundation of China (No. 51575302).

References

1. Bo, C.: The development and use of machine tools in historical perspective. *J. Econ. Behav. Organ.* **5**(1), 91–114 (1983)
2. Robotworx: History of industrial robots [EB/OL], 22 November 2013. <http://www.robots.com/education/industrialhistory>
3. Jone, M.: A brief history of awesome robots [EB/OL], 02 June 2013. www.motherjones.com/media/2013/05/robots-modern-unimate-watson-roomba-timeline

4. Reinholtz, V.A., Watson, L.T.: Enumeration and Analysis of Variable Geometry Truss Manipulators (1990)
5. Murthy, V., Waldron, K.J.: Position kinematics of the generalized lobster arm and its series parallel dual. *Trans. ASME J. Mech. Des.* **114**, 406–413 (1992)
6. Kraus, J.: Variable structure position control of an industrial robotic manipulator. *J. Braz. Soc. Mech. Sci.* **8**, 23–25 (2002)
7. Lee, H.Y., Roth, B.A.: Closed-form solution of the forward displacement analysis of a parallel mechanisms. In: *Proceedings of the IEEE International Conference on Robotics and Automation* (1993)
8. Miura, K.: Variable Geometry Truss Concept. The Institute of Space and Astronautical Science. Report NO. 614, September 1984
9. Suzuki, K., Maeda, Y., Ishibashi, Y., Fukushima, N.: Improvement of operability in remote robot control with force feedback. In: *2015 IEEE 4th Global Conference on Consumer Electronics (GCCE)* (2015)
10. Fang, H., Fang, Y., Hu, M.: Forward position analysis of a novel three DOF parallel mechanism. In: *Proceedings of the 11th World Congress in Mechanism and Machine Science*, Tianjin, China, 1–4 April 2004, pp. 154–157. China Machinery Press, Beijing (2004)
11. Wei, G., Chen, Y., Dai, J.S.: Synthesis, mobility, and multifurcation of deployable polyhedral mechanisms with radially reciprocating motion. *J. Mech. Des. Trans. ASME* **136**(9), 091003 (2014)
12. Zhao, J.S., Chu, F., Feng, Z.J.: The mechanism theory and application of deployable structures based on SLE. *Mech. Mach. Theor.* **44**(2), 324–335 (2009)
13. Yang, Y., Jiang, B., Hu, S.: Fast trajectory planning for VGT manipulator via convex optimization. *Int. J. Adv. Robot. Syst.* **12**(9), 1 (2015)
14. Chettibi, T.: Synthesis of dynamic motions for robotic manipulators with geometric path constraints. *Mechatronics* **16**(9), 547–563 (2006)
15. Lin, F.Y.: Optimal motion planning for robotic manipulators. *Adv. Mater. Res.* **902**, 262–266 (2014)